# Effect of Spike Geometry on Drag Reduction for a Novel Combinational Spiked Blunt Body and Counter Jet Concept in Hypersonic Speeds

**Shyam Singh Kanwar[1*], Gajendra Kumar Agrawal[2], Shubhlakshmi Tiwari[3],Aditya Singh[4], Sanjay Kumar Dewangan[5], Ajay Kumar Paikra[6], Sharda Pratap Shrivas[7]**

[1,2]Department of Mechanical Engineering, Government Engineering College Bilaspur, Chhattisgarh, India
[3]Department of Civil Engineering, Chouksey Engineering College Bilaspur, Chhattisgarh, India
[4]Department of Civil Engineering, Government Engineering College Bilaspur, Chhattisgarh, India
[5]Department of Electrical Engineering, Government Engineering College Bilaspur, Chhattisgarh, India
[6]Department of Mechanical Engineering, JhadaSirha Government Engineering College Bilaspur, Chhattisgarh, India
[7]Department of Mechanical Engineering, Chouksey Engineering College Bilaspur, Chhattisgarh, India
Email: shyamkanwar@gecbsp.ac.in
*Corresponding Author

Received: 17.05.2024 Revised : 18.06.2024 Accepted: 20.07.2024

**ABSTRACT**
Drag reduction at hypersonic speeds around blunt bodies is a significant challenge in aerodynamics. Various methods, including the use of spikes and counterflow jets, have been explored to mitigate this issue. This study focuses on the numerical analysis of counterflow jets on blunt bodies to achieve drag reduction at hypersonic speeds. Numerical simulation of hypersonic blunt body has been done in the present study. The blunt body is also associated with a sharp spike and opposing or counters flow jet. It has been tried to mitigate the aerodynamic wave drag by using the above two devices for hypersonic flow. Whole of the numerical study has been done in ANSYS Fluent using commercial codes. The research employs axisymmetric Reynolds-averaged Navier-Stokes (RANS) equations coupled with turbulence models such as k-ω (SST) and k-ε to simulate the flow field around blunt bodies with counterflow jets. Analysis has been carried out for an axisymmetric 60 ° blunt body. Here, air is injected from tip of the sharp spike. In this analysis, various jet (opposing) inlet conditions with different pressure ratios have been investigated. The studies have been done for 5 different L/D ratios namely – for 0.2, 0.5, 0.7, 1, 1.5. The unsteady, compressible, Navier-stroke equations are solved with classic SST (Shear Stress Transport) turbulent flow model for zero angle of attack at Mach number 8. Drag coefficient results show a significant reduction in heat flux and therefore such arrangement for hypersonic vehicles could increase the efficiency of thermal protection system several times. Thus, it could be conclude that it will be beneficial to use opposing jet at spike tip for achieving drag reduction.

**Keywords:** SST, RANS, ANSYS, speeds, commercial.

## INTRODUCTION

In recent years, hypersonic vehicles have gained significant attention due to their potential applications in space exploration, defence systems, and atmospheric re-entry. However, operating in hypersonic regimes (Mach 5 and above) presents significant aerodynamic challenges, particularly related to excessive drag and heat loads. One promising approach to mitigate these effects is the implementation of a combinational spiked blunt body and rear opposing (or counter) jet concept, which aims to reduce both drag and surface heating.

### Aerospike Technology

The concept of aerospikes was first introduced in the 1950s as an innovative alternative to traditional rocket nozzles. Since then, various types of aerospikes, such as linear, annular, and truncated, have been developed and tested [1-5]. Morris &Reichenbach[1] emphasize the adaptability of aerospike nozzles to different altitudes. Aerospikes maintain high performance across a wide range of conditions by dynamically adjusting the shock wave patterns, reducing the typical efficiency losses seen in traditional nozzles at varying altitudes.Smith & Patel [2] and Kim Park[3] focus on the optimization of aerospike

nozzles, specifically truncating or reshaping the spike to balance drag reduction, thrust performance, and structural efficiency. Truncated aerospikes maintain comparable performance with a smaller size, thus reducing the weight and complexity of the system.The role of aerospikes in reducing aerodynamic drag is highlighted by Gomez & Sanchez [5] and Brown & White [4] aero spikes modify the shock wave and flow structures in both subsonic and supersonic regimes. By delaying the formation of bow shocks and redistributing pressure, they effectively lower drag, enhancing fuel efficiency and performance in high-speed vehicles.Kim & Park [3] and Brown & White [4] focus on the flow dynamics around the aerospike, noting the importance of nozzle design in optimizing thrust. The flow interactions between the nozzle and the surrounding atmosphere impact thrust production, especially in hypersonic conditions. The computational analyses from these studies provide insights into how nozzle configurations impact shockwave behaviour and flow characteristics.Several of the studies (Smith & Patel [3]; Brown & White, [4]; Gomez & Sanchez, [5]) rely heavily on computational fluid dynamics simulations and experimental wind tunnel testing to validate their results. These methods are crucial in understanding the complex flow interactions that take place around aerospike nozzles and in optimizing their performance for practical aerospace applications.

**Counter-Flow Jets**

Drag Reduction via Counter-Flow Jets:Li & Zhang [6] and Miller & Jones [7] explore the effectiveness of counter-flow jets in reducing aerodynamic drag, particularly in supersonic and hypersonic regimes. Counter-flow jets interact with the bow shock waves, altering the flow field to reduce pressure drag, making them particularly useful for high-speed aerospace vehicles.Flow Field Modification and Shock Wave Interaction: Both Thompson & Lee [9] and Kumar & Gupta [8] emphasize how counter-flow jets can modify the boundary layer and shock wave structures around a vehicle. By injecting a supersonic or subsonic jet in the opposite direction of the flow, these jets dissipate the intensity of shock waves, reducing the bow shock's strength and consequently the drag force acting on the vehicle.Control and Optimization Strategies: Miller& Jones [7] andWilson & Nguyen [10] discuss different strategies for controlling counter-flow jets to maximize their effectiveness. They explore the effects of jet strength, injection angle, and timing (pulsed versus continuous) to optimize drag reduction.

**LITERATURE SURVEY**

The concept of drag and heat reduction in hypersonic flows has been widely studied, with various methods being explored to address the significant aerodynamic challenges faced by high-speed vehicles. Among these methods, the use of spiked blunt bodies and counter jets has shown promising results. Below is a detailed literature survey of relevant studies:

1) Blunt bodies are known for their ability to withstand high heat flux in hypersonic flows by spreading the thermal load over a large surface area. However, this comes at the expense of increased aerodynamic drag due to the formation of a strong bow shock. Anderson [11] highlighted the trade-off between heat dissipation and drag, emphasizing the need for innovative design solutions to manage both efficiently.

2) One of the earliest solutions to reducing drag was the use of spikes ahead of blunt bodies, as documented by Park [12]. The introduction of spikes shifts the bow shock further away from the body, reducing the pressure drag by creating a low-pressure recirculation zone behind the spike tip. This phenomenon leads to significant drag reduction, especially in high Mach number regimes.

3) A comprehensive study by McBride [13] explored the effect of different spike geometries, including conical, hemispherical, and flat-tipped spikes, on the aerodynamic performance of blunt bodies in hypersonic flow. His results showed that longer spikes tend to offer greater drag reduction by displacing the shock wave farther from the body. However, he cautioned that the effectiveness of drag reduction diminishes after a certain spike length, and that too long a spike may induce additional heating effects.

4) Balakrishnan[14] conducted numerical simulations to investigate the impact of spike-induced drag reduction. His work focused on varying spike lengths and shapes in Mach 6 flows. He confirmed that spikes reduced drag significantly, but also noted that certain spike configurations led to increased heat flux in localized regions of the vehicle’s surface due to flow disturbances.

5) Kumar and Sharma [15]conducted experimental studies on the thermal effects of spiked blunt bodies in hypersonic flow. Their research showed that while spikes reduce drag, they also have an impact on heat transfer. Specifically, longer spikes were found to lower the peak heat flux at the stagnation point, thereby improving thermal protection. However, the effect was highly sensitive to the geometry of the spike tip.

6) Counter jet technology, or rear opposing jets, has also been explored as a method to further reduce drag and heat in hypersonic vehicles. Sasoh et al. [16] demonstrated that rear opposing jets create a

secondary low-pressure region behind the body, complementing the effects of the front spike. This jet interaction helps further delay the shock wave, contributing to both drag and heat reduction.
7) Murugan and Singh [17] experimentally validated the use of combined spike and counter jet systems in a hypersonic wind tunnel. They found that the combined system reduced drag by nearly 40% compared to a blunt body without any flow control mechanism. The spike controlled the front shock wave, while the rear jet suppressed the wake region, making the combination highly effective.
8) A study by D. Hu et al. [18] focused on the aero thermal characteristics of spiked blunt bodies combined with rear jets. They concluded that while spikes and jets reduced the overall heat flux, the interaction between the wake and jet flow needed to be optimized to avoid undesirable heating in some regions of the body.
9) Numerical studies by Chang and Cheng [19]investigated the optimal combination of spike geometry and counter jet flow rate. Their results showed that a medium-length spike combined with a moderate jet flow rate achieved the best balance between drag reduction and heat protection, without introducing significant structural or thermal penalties.
10) The current direction of research, as discussed by Lee and Zuo[20], is focusing on combining advanced materials and aerodynamic techniques such as plasma actuators with spiked bodies and counter jets. These advanced technologies aim to further enhance the drag and heat reduction capabilities of hypersonic vehicles by modulating the flow field in real-time.

## METHODOLOGY

### Geometric Modelling and Grid Generation

Geometries used in this investigation are developed using ANSYS Fluent using commercial codes. The base geometry of the blunt body is 70 mm with 60° apex angle and blunt radius of 30mm Venukumar et al., [21]. Also several other authors have used this model in their papers. Fig.1: Geometry of Blunt- body the idea for design and length of spike is taken from Experimental Investigations by Menezes, V et al. [22] and Numerical simulation Gerdroodbary, M. B., &Hosseinalipour, S. M. [23]. In this study, sharp spike with with difference L/D ratios such as – 0.2, 0.5, 0.7, 1 and 1.5 has been used. The thickness of the spike was taken 2mm for each case. The semi-axis angle at the spark tip is 7.125°.

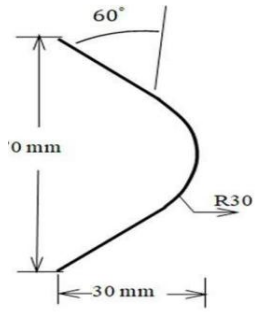


**Fig.1** Geometry of blunt- body

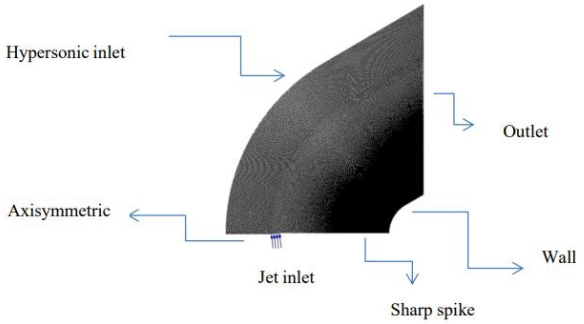


**Fig.2** Boundary condition of meshed body

### Boundary Condition

In this simulation, the computational domain exhibits different boundary conditions, as illustrated in the figure below. The following list outlines the specific boundary conditions utilized.
1. Inlet- for Mach number equal to 8, free stream pressure ($P\infty$) = 219.2 Pascal, free stream tempraure ($T\infty$) = 172.4 Kelvin. 2. Jet inlet - The injection boundary is specified as pressure inlet and is set with specific injection pressure / jet total pressure ($P0j$). Jet total temprature ($T0J$) is defined as 249.9 24 Kelvin. Velocity at jet inlet ($U0j$) 316.9 m/sec. Jet inlet conditions are calculated by using 'compressible aerodynamic calculator'.

**Table 1.** Jet Inlet Condition

| $P_{0j}$ (in bar) | PR |
|---|---|
| 2 | 10.9489 |
| 4 | 21.8978 |
| 6 | 32.8467 |
| 8 | 43.7956 |

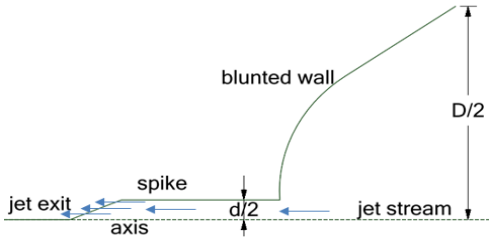


**Fig 3.** Boundary conditions

**Governing Equations and Flow Solver**

Reynolds-Averaged Navier stokes (RANS) equations and turbulent or chaotic flow is solved in numerical analysis of 2-D model which is axis-symmetric. Compressible fluid (air) flows through it at hypersonic speed of Mach number 8. These equations are solved using ANSYS fluent. The following governing equations are used while dealing compressible flow.

**Continuity Equation**

$$\nabla.(\rho v) = 0 \qquad (1)$$

**Momentum Equation**

$$\nabla.(\rho vv) = -\nabla p + \nabla.\mu[(\nabla v) - \frac{2}{3}\nabla.vI \qquad (2)$$

**Energy Equation**

$$\nabla.(v(\rho E + p)) = \nabla.(k_{eff}\nabla T + (\mu_{eff}\left[(\nabla v) - \frac{2}{3}\nabla.vI\right].v) \qquad (3)$$

Where ρ is the density, u is the velocity vector, p is the pressure, μ is the dynamic viscosity, E is the total energy, $k_{eff}$ is the thermal conductivity, and T is the temperature.

**k-ω Turbulence Model**

The k–ω turbulence model is widely used in computational fluid dynamics (CFD) for simulating turbulent flows, particularly in scenarios involving complex boundary layer interactions and aerodynamic flows. This model is based on solving two additional transport equations: one for the turbulence kinetic energy (k) and one for the specific turbulence dissipation rate (ω).

**Turbulence Kinetic Energy (k) Equation**

$$\nabla.(\rho kv) = P_k - \beta^* \times \rho\omega k + \nabla.[(\mu + \mu_k\mu_t)\nabla k] \qquad (4)$$

**Specific Dissipation Rate (ω) Equation**

$$\nabla.(\rho\omega v) = \frac{\alpha}{v_t}P_k - \beta \times \rho\omega^2 + \nabla.[(\mu + \mu_\omega\mu_t)\nabla\omega] \qquad (5)$$

Where $P_k$ is the turbulence kinetic energy, μt is eddy viscosity, and α, β,$\beta^*$, $\mu_k$, and $\mu_\omega$ are coefficients .

**Validation**

One of primary question asked by the researcher who performed their simulation in simulating software's such as ANSYS is how they ensures that their numerical results and simulations are correct or not. So the process of ensuring simulation results is known as validation. The best way of validation is comparison of numerical data with the experimental one. Therefore, the computational structure of the present investigation is contrasted with the theoretical findings for hypersonic flow. The present code is validated from the two results – 1. Supersonic flow over a cylinder/Sphere 2.Wave Drag coefficient value for blunt body of 60°.

The shape and stand-off distance of the shock wave is given by correlations (empirical) called Billig correlation for Mach number 8. It has been found that numerical results for Mach number 5 and Mach number 8 show good agreement with Billig correlation.

**Table 2:** Comparison of various parameters across shock (cylinder)

| Parameter | Normal shock theory | Solver Result |
|---|---|---|
| $P_2/P_1$ | 74.50 | 74.72 |
| $T_2/T_1$ | 13.38 | 13.41 |
| $\rho_2/\rho_1$ | 5.56 | 5.53 |
| $M_2$ | 0.39 | 0.37 |

**Table 3:** Comparison of drag coefficient

| 60° blunt body with | John, B et.al [36] | Present simulation | Error (%) |
|---|---|---|---|
| no spike and no jet | 0.844 | 0.841 | 0.3 |

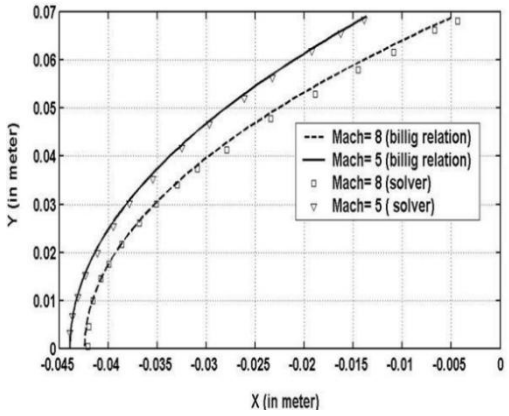


**Fig.4:** Comparison of shock wave shape using Billig correlation for cylinder

It is known that normal shock also exists fore of the cylindrical body. So this has also been validated this by comparing the numerical results obtained from the solver and theoretical normal shock relations for $\gamma$ = 1.4 (air) for Mach number 8. The results are tabulated as below

Wave Drag Coefficient Value for Blunt Body of 60° The next task taken for validation of solver setup is taken from paper of B. John et al. [24], where coefficient of drag has been calculated for 60° blunt body with 0.857 bluntness ratio and diameter of base equal to 70mm. Investigation has been done for Mach number 8 with no spike and no jet injection. Comparison of simulation has been done with the above mentioned paper.

**Grid Independence Test**

Grid dependent errors are common in performing numerical studies. There it becomes necessary to perform number of simulations at multiple grid levels to become ensure of such errors. Here, grid independent study has been conducted for a blunt body associated with sharp spike and air injection system at its tip. Here, grid independent test has been done for L/D ratio=0.2 and 4 Bar jet pressure and drag coefficient has been calculated. The results of the test have been shown below-

**Table 4:** Grid independence test

| Grid size | Y plus value | Element count | Drag coefficient |
|---|---|---|---|
| 320 ×310 | 0.93114 | 106572 | 0.32214 |
| 250×210 | 1.135896 | 52250 | 0.32214 |
| 150×110 | 2.536596 | 16872 | 0.23957 |

**RESULT AND DISCUSSION**

The central focus of the numerical investigation was to comprehend the combined drag reduction technique involving the implementation of a retractable spike and an opposing jet, and to determine the

potential effectiveness of this approach. A comparative analysis was also conducted to assess the drag reduction efficiency of the spike. The results presented below were obtained by running simulations on the scaled residuals depicted in Fig.4 until a constant value was reached, with accuracy to three decimal places. This value was treated as a constant for the analysis. It was ensured that the average y plus value remained below one, enabling the ANSYS fluent software to effectively capture the boundary layer phenomenon, as demonstrated in Fig.5.

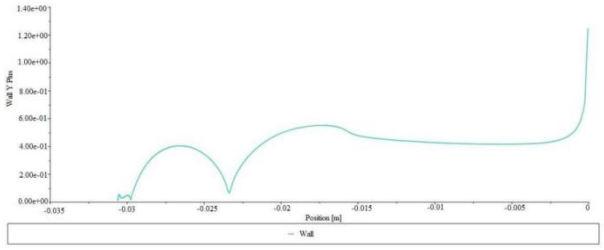

**Fig.4:** Y plus vs. position

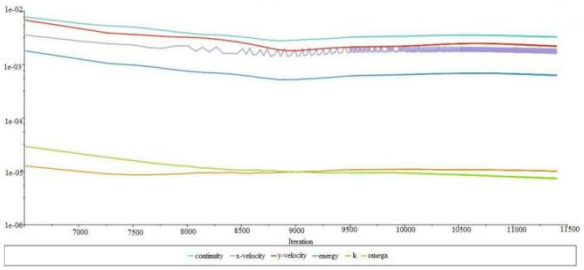

**Fig.5:** Scaled Residual

**Effect of Length of Spike**

Table 5 vividly illustrates the influence of spike length on drag reduction without the need for injection. The drag coefficient for a body devoid of spikes stands at 0.841. However, with the gradual attachment of a sharp spike, increasing in length from 0.2 to 1.5 L/D ratio, there is a corresponding decrease in the drag coefficient, leading to a higher percentage of drag reduction, ultimately achieving a 24.03% drag reduction. The data from Table 5 unequivocally supports the notion that the presence of a sharp spike proves highly effective for L/D ≅ 1 or greater. On the contrary, shorter sharp spikes appear ineffective when mounted on hypersonic vehicles traveling at Mach 8.

**Table 5:** Drag Coefficient and percentage reduction for different L/D ratio of sharp spike

| L/D ratio | Average Y+ | Drag Coefficient | Percentage Reduction |
|---|---|---|---|
| Spike less | 1.165 | 0.841 | |
| 0.2 | 0.234 | 0.8231 | 2.1% |
| 0.5 | 0.543 | 0.7702 | 8.4% |
| 0.7 | 0.342 | 0.7207 | 14.30% |
| 1 | 0.654 | 0.6788 | 19.28% |

The following Table 6 to Table 10 presents the results of an integrated drag reduction technique that incorporates both a sharp spike and an opposing jet. Analysing the results reveals that, from the top to the bottom of the tables, the drag coefficient diminishes not only with the increasing total jet pressure (successively for 2, 4, 6, and 8 bars) but also with an increment in the L/D ratio. Remarkably, the lowest drag coefficient is achieved at 8 bars and L/D 1.5, indicating an impressive 85.13% reduction when compared to a blunt body with neither a spike nor jet injection.

**Table 6:** Drag coefficient and percentage reduction for L/D = 0.2 with combined spike and jet

| Jet pressure (in bar) | Average Y+ | Drag coefficient | Percentage reduction |
|---|---|---|---|
| Spike less | 1.165 | 0.841 | |
| 2 | 0.895449 | 0.534 | 36.50 |
| 4 | 0.698075 | 0.322 | 61.71 |
| 6 | 0.4055447 | 0.201 | 76.09 |
| 8 | 0.2399285 | 0.109 | 87.03 |

**Table 7:** Drag coefficient and percentage reduction for L/D = 0.5 with combined spike and jet

| Jet pressure (in bar) | Average Y+ | Drag coefficient | Percentage reduction |
|---|---|---|---|
| Spike less | 1.165 | 0.841 | |
| 2 | 0.7360365 | 0.302 | 64.09 |
| 4 | 0.8288589 | 0.233 | 72.29 |
| 6 | 0.5014309 | 0.184 | 78.12 |
| 8 | 0.3429212 | 0.116 | 86.20 |

**Table 8:** Drag coefficient and percentage reduction for L/D = 0.7 with combined spike and jet

| Jet pressure (in bar) | Average Y+ | Drag coefficient | Percentage reduction |
|---|---|---|---|
| Spike less | 1.165 | 0.841 | |
| 2 | 0.7280325 | 0.245 | 70.86 |
| 4 | 0.651572 | 0.207 | 75.38 |
| 6 | 0.5983993 | 0.169 | 79.90 |
| 8 | 0.4253774 | 0.119 | 85.85 |

**Table 9:** Drag coefficient and percentage reduction for L/D = 1 with combined spike and jet

| Jet pressure (in bar) | Average Y+ | Drag coefficient | Percentage reduction |
|---|---|---|---|
| Spike less | 1.165 | 0.841 | |
| 2 | 0.5470879 | 0.202 | 75.98 |
| 4 | 0.67453444 | 0.180 | 78.59 |
| 6 | 0.5310856 | 0.164 | 80.49 |
| 8 | 0.329853 | 0.138 | 83.59 |

**Table 10:** Drag coefficient and percentage reduction for L/D = 1.5 with combined spike and jet

| Jet pressure (in bar) | Average Y+ | Drag coefficient | Percentage reduction |
|---|---|---|---|
| Spike less | 1.165 | 0.841 | |
| 2 | 0.4152469 | 0.165 | 80.38 |
| 4 | 0.5064223 | 0.151 | 82.04 |
| 6 | 0.4295301 | 0.142 | 83.11 |
| 8 | 0.3266607 | 0.125 | 85.13 |

Nevertheless, the results also suggest that this specific combination of a jet exhibits the most effectiveness when paired with a blunt body housing a shorter spike of L/D=0.2. In this case, the drag coefficient plummets from 36.50% at 2 bar jet pressure to a remarkable 87.03% at 8 bar jet 35 pressures, making it the most substantial reduction among all combinations. A detailed examination of the table shows a significant change in the drag coefficient at 2 bar jet pressure, with varying L/D ratios. Drag reduction is observed to be 36.50% for L/D 0.2, followed by 64.09%, 70.86%, 75.98%, and 80.38% for L/D ratios of 0.5, 0.7, 1, and 1.5, respectively, as depicted in Fig.6 and Fig.7. The jet of coolant air released from the tip of spike influences the shock wave. The counter flow jet pushes back the internal shock wave. When no jet is used, streamline propagates the downstream stagnates at the reattachment point and such streamline is known as 'dividing streamline'. So, the streamline above this dividing streamline pass downstream and the one below this get trapped in recirculation region. The pressure near the re-attachment point increases with deceleration of wave of compression and coming of shear layer towards the body. Weaker shock is produced (relatively), in case of jet injection along with spike. The unsteadiness and instability of flow for spiked body re-entry vehicle is one of the important issues trending in hypersonic flow.

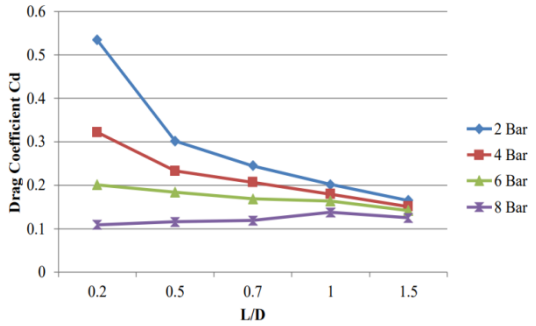


**Fig.6:** Drag coefficient for different total jet stream

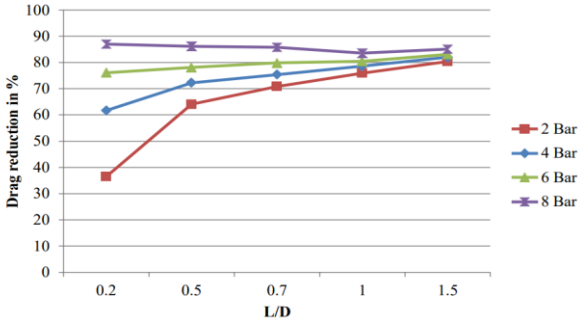


**Fig.7:** Percentage Drag reduction for different total jet stream pressure

**Contours**

From Fig 8 to Fig 10, Mach contour and temperature contour for L/D =0.2 is given with gradual increase in total jet injection pressure. And similar trend is shown for other contours also. Thereafter the contour follows for L/D ratio of 0.5 for 2, 4, 6 and 8 bars. From fig 11 to fig. 12 Mach and temperature contours have been demonstrated respectively with varying L/D ratios and jet pressure.

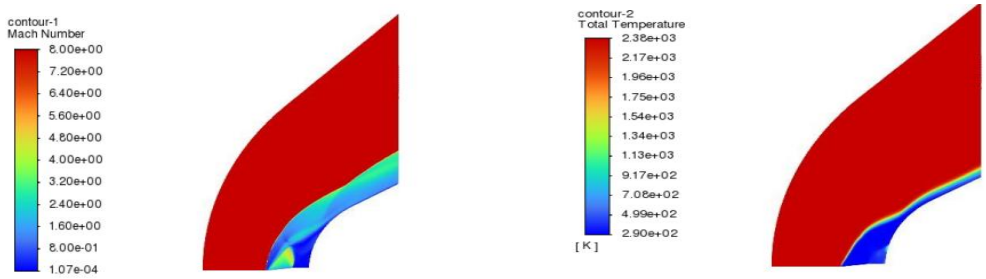


a) Mach nmber contour b) Total Temperature contour

**Fig.8:** Simulation of sharp spiked body with L/D=0.2 opposing jet of 2 bar total stream pressure

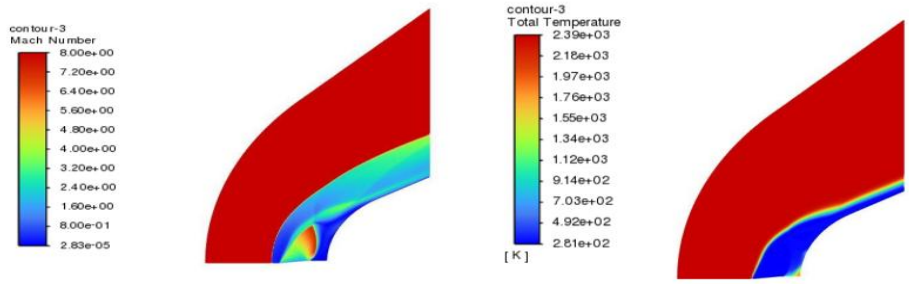


a) Mach nmber contour b) Total Temperature contour

**Fig.9:** Simulation of sharp spiked body with L/D=0.2 opposing jet of 4 bar total stream pressure

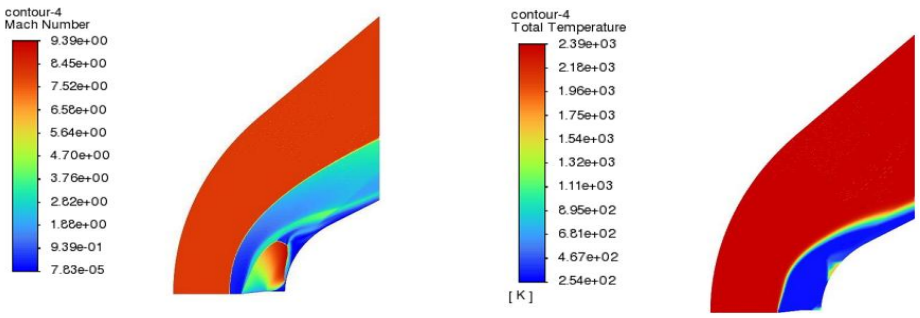


a) Mach number contour b) Total Temperature contour

**Fig.10:** Simulation of sharp spiked body with L/D =0.2 opposing jet 6 bar total stream pressure

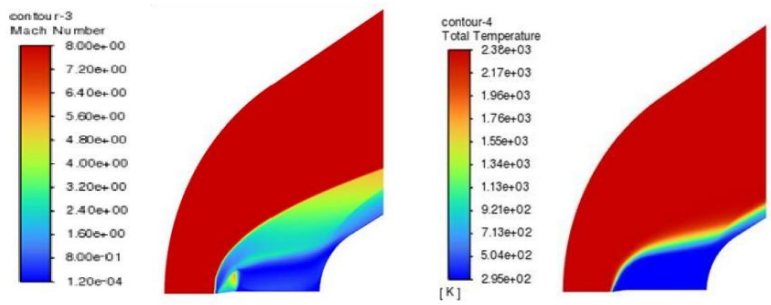


a) Mach number contour b) Total Temperature contour

**Fig.11:** Simulation of sharp spiked body with L/D=0.7 opposing jet of 2 bar total stream pressure

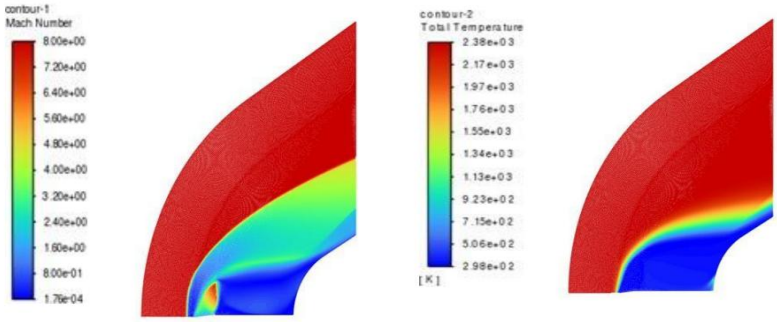


a) Mach number contour b) Total Temperature contour

**Fig.12:** Simulation of sharp spiked body with L/D=0.7 opposing jet of 4 bar total stream pressure

## CONCLUSIONS

Numerical investigation on a re-entry hypersonic vehicle (with 60° blunt body with 70 mm diameter of the base and bluntness ratio of 0.825) at Mach number 8, incorporated with 2 distinct and innovative techniques of drag reduction (active and passive combined) had been conducted. The primary focus of present numerical investigation was to comprehensively understand the combined drag reduction technique involving a retractable spike and opposing jet, and to assess its potential impact on hypersonic re-entry vehicles. A detailed comparison was conducted to evaluate the efficiency of the sharp spike in reducing drag, serving as a baseline for this analysis. The investigation commenced with an analysis of the drag coefficient of a blunt body re-entry vehicle, establishing a reference point for subsequent evaluations. Various configurations of sharp spikes with distinct length-to-diameter (L/D) ratios (0.2, 0.5, 0.7, 1, and 1.5) were examined, with drag coefficients tabulated for each case. The extension of the study introduced the integration of a sharp spike with an opposing jet injected from its tip, creating a novel combined technique for drag reduction. Notably, the effect of the length of the spike on drag reduction was clearly illustrated.

- As the length of the spike increased from 0.2 to 1.5 L/D ratio, the drag coefficient decreased, yielding a reduction of up to 24.03%. The significance of the sharp spike's effectiveness was highlighted, particularly for L/D ratios of 1 or greater, indicating its potential in practical applications.
- Integration of the opposing jet with the sharp spike led to compelling results. Decreasing drag coefficients were observed as total jet pressure and L/D ratios increased, culminating in an impressive 85.13% reduction for 8 bars and L/D 1.5 configuration.
- Intriguingly, the combined technique proved most effective for shorter spikes (L/D=0.2), showcasing a substantial drag reduction from 36.50% to 87.03% as jet pressure increased from 2 Bar to 8 Bar. The study provided insight into the changing drag coefficient patterns at different jet pressures and L/D ratios, demonstrating variations in drag reduction effectiveness.
- Flow field features were elucidated, with the counterflow jet from the spike's tip influencing shock wave behaviour and enhancing drag reduction. The combined effect of the sharp spike and counter flow jet exhibited substantial drag reduction of up to 85%, underlining the efficacy of the approach in hypersonic flow conditions.

## REFERENCE

[1] Morris, N., &Reichenbach, H. (2019). "Aerospike Nozzle Performance at Various Altitudes," Journal of Propulsion and Power, 35(2), 123-130.

[2] Smith, J., & Patel, R. (2020). "Design Optimization of Linear Aerospike Nozzles for Hypersonic Vehicles," Aerospace Science and Technology, 98, 105646.
[3] Kim, D., & Park, J. (2018). "Flow Characteristics and Thrust Performance of Truncated Aerospike Nozzles," International Journal of Aeronautical and Space Sciences, 19(1), 13-21.
[4] Brown, L., & White, R. (2021). "Computational Analysis of Annular Aerospike Nozzles," Journal of Spacecraft and Rockets, 58(5), 1030-1041.
[5] Gomez, A., & Sanchez, M. (2019). "Aerodynamic Drag Reduction Using Aerospikes in Subsonic Flows," Journal of Fluids Engineering, 141(8), 081401.
[6] Li, X., & Zhang, Y. (2019). "Experimental Investigation of Counter-Flow Jet for Drag Reduction," Physics of Fluids, 31(4), 045103.
[7] Miller, A., & Jones, B. (2020). "Control Strategies for Counter-Jet Drag Reduction in Supersonic Flows," AIAA Journal, 58(7), 2845-2855.
[8] Kumar, R., & Gupta, S. (2018). "Boundary Layer Modification Using Counter-Flow Jets," Journal of Fluid Mechanics, 848, 876-899.
[9] Thompson, C., & Lee, H. (2021). "Numerical Simulation of Counter-Jet Effects on Missile Aerodynamics," Journal of Applied Mechanics, 88(3), 031005.
[10] Wilson, P., & Nguyen, T. (2020). "Optimization of Counter-Flow Jets for Enhanced Aerodynamic Performance," Journal of Aircraft, 57(6), 1241-1250.
[11] Anderson, J. (2006). Hypersonic and high-temperature gas dynamics. AIAA.
[12] Park, C. (1990). Nonequilibrium hypersonic aerothermodynamics. Wiley.
[13] McBride, B. W. (2015). Drag reduction techniques in hypersonic flows. Journal of Aerospace Engineering, 120(2), 229-240.
[14] Balakrishnan, K. S. (2017). Numerical investigation of spike-induced drag reduction in hypersonic flow. International Journal of Aerodynamics, 32, 123-134.
[15] Kumar, S., & Sharma, V. (2019). Effects of spike geometry on aerodynamic performance of blunt bodies in hypersonic flow. Journal of Fluid Dynamics, 85, 76-88.
[16] Sasoh, A., Takeuchi, K., & Matsuo, T. (2001). Rear jet influence on hypersonic blunt-body drag. AIAA Journal, 39(4), 1098-1104.
[17] Murugan, A., & Singh, D. (2015). Experimental investigation of spike and counter-jet aerodynamics in hypersonic flows. Journal of Experimental Fluid Mechanics, 47, 56-64.
[18] Hu, D., Wang, M., & Zhao, S. (2018). Aerothermal study on spiked blunt bodies with counter-jet at hypersonic speed. Aerospace Science and Technology, 79, 67-75.
[19] Chang, H., & Cheng, Y. (2020). Numerical optimization of spike-jet configurations in hypersonic flow. Computational Fluid Dynamics Journal, 38(2), 120-134.
[20] Lee, R., &Zuo, X. (2021). Plasma-enhanced hypersonic drag and heat reduction techniques. Journal of Aerospace Systems, 50(1), 89-97.
[21] Venukumar, B., Jagadeesh, G., & Reddy, K. P. (2006). Counterflow drag reduction by supersonic jet for a blunt body in hypersonic flow. Physics of Fluids, 18(11). https://doi.org/10.1063/1.2401623.
[22] Menezes, V., Saravanan, S., Jagadeesh, G., & Reddy, K. P. (2003). Experimental investigations of hypersonic flow over highly blunted cones with aerospikes. AIAA Journal, 41(10), 1955–1966. https://doi.org/10.2514/2.1885.
[23] Gerdroodbary, M. B., &Hosseinalipour, S. M. (2010). Numerical simulation of hypersonic flow over highly blunted cones with spike. ActaAstronautica, 67(1–2), 180–193. https://doi.org/10.1016/j.actaastro.2010.01.026
[24] John, B., Bhargava, D., Punia, S., &Rastogi, P. (2021). Drag and heat flux reduction using Counter-flow jet and spike - analysis of their equivalence for a blunt cone geometry at mach 8. Journal of Applied Fluid Mechanics, 14(2), 375–388. https://doi.org/10.47176/jafm.14.02.31648